

ESTIMATION OF WILDFIRE SPREAD RATE FROM GEOSTATIONARY SATELLITE DATA

Xiangzhuo Liu^a, Binbin He^{*a b}, Xingwen Quan^a, Chongbo Wen^a, Xiaofang Liu^c

^a School of Resources and Environment,
University of Electronic Science and Technology of China, Chengdu, Sichuan 611731, China;

^b Center for Information Geoscience,
University of Electronic Science and Technology of China, Chengdu, Sichuan 611731, China;

^c School of Computer Science, Sichuan University of Science and Engineering, Zigong 643000, China;

* Corresponding author. E-mail: binbinhe@uestc.edu.cn.

ABSTRACT

Fire Spread Rate (FSR) is one of the key factors for fire rescue and prevention. Remote sensing images have an advantage of acquiring intuitive information timely. To achieve extracting real-time FSR from remote sensing data, a method based on the movement rate of burned area centroid is presented in this study. The FSR extracted from geostationary Himawari-8 (H-8) data in two bushfires outbreak in Esperance, Western Australia in 2015. And the FSR estimated from CSIRO (Commonwealth Scientific and Industrial Research Organization) Grassland Fire Spread Model (CGFSM) were set as the benchmark to assess the presented approach. The results illustrated that the proposed method yield a promising accuracy by comparing with the FSR from CGFSM in that two fires, with the coefficient of determination (R^2) reaches to 0.76 and root-mean-square error (RMSE) is $0.50 \text{ m}\cdot\text{s}^{-1}$. Furthermore, this study provides a potential application of geostationary satellite in extracting real-time wildfire behavior.

Index Terms— Himawari-8, Real-time, Fire Spread Rate (FSR), Centroid, CSIRO Grassland Fire Spread Model (CGFSM)

1. INTRODUCTION

Wildfire is one of the natural disasters that cause a lot of issues in economy, environment and society [1, 2]. The research of wildfire can be mainly divided into the following three parts: the prediction before fire, the information extraction during fire and the recovery of vegetation after fire. At present, there have been many types of research on the pre-disaster and post-disaster using remote sensing data. However, the information extraction from the remotely sensed data in the process of fire is less involved[3]. The extraction of information during the firing contains the spread rate and direction of the fire, the duration of the fire, that is, the beginning and ending time of the fire. Estimation of the fire spread rate and direction is important for firefighter rescue and evacuation of personnel, which can reduce casualties and economic losses. Besides, extraction of real-time fire rate is

very significant in fire monitoring and management.

There are mainly two approaches for estimating FSR, empirical statistical model and physical model. In empirical approaches, observed data from the field or indoor experiment was used to establish the formulas among the FSR, fuel content and meteorological data [4, 5]. These methods are simple and computationally efficient, which have been widely used in practice [6]. Many empirical models had been developed range from grasslands to shrublands and forests[7]. However, these methods are normally site and sensor specific, which have low robustness and only suitable for specific plants [8]. Physical models take the mechanism of fire propagation into consideration, which combine thermodynamics, air-dynamics and botany[6] together. To solve the balance equations of the conservation of energy and momentum, the calculations are usually time-consuming, and as a result, few models have been proposed. Both empirical and physical model need mounts of observation data in the process of model generation. In field or experiment, ocular observation, visible or infrared spectrum images and thermocouple instruments are always used to obtain fire spread rate of fine scale fires.

Due to the time resolution and data quality of the solar orbit satellite data, researches about real-time fire rate extraction based on time series remote sensing images are rare. Douglas A[9] had extracted the FSR from the repeat pass Airborne Thermal Infrared (ATIR) imagery by capturing the spread vectors and units in 2002 Williams fire. Pastor[10] had proposed a method to compute the spread rate of linear flame fronts by thermal image processing. Those methods all have limitations in time and spatial resolution.

The launches of Himawari-8, a geostationary satellite with time resolution of ten minutes, making real-time monitor and detection of fire behaviors possible. Fatkhuroyan et al. [11] successfully detected the forest fires in Indonesia on August-October 2015 using H-8 data. Xu et al. [12] applied the geostationary Fire Radiative Power(FRP) algorithm designed for the Meteosat SEVIRI to H-8. Their results showed that H-8 have better performance compared with other geostationary sensors, such as FY-2 and MTSAT. Wickramasinghe et al. [13] added the Near Infrared(NIR) and red reflectance to traditional active fire detection algorithms,

designed the Multi-Spatial Resolution Approach for H-8, which could map fire lines with a 500m resolution. Guang et al. [14] also presented an easy-running algorithm to detect and track real-time wildfire in Australia. Moreover, H-8 was also used to retrieve the near real time Sea Surface Temperature(SST) through NOAA Advanced Clear-Sky Processor for Ocean (ACSPO) system [15].

To date, there are no authority active fire algorithms for H-8. This is the first study on the estimation of the FSR from the H-8 data. For that end, a method based on the movement rate of burned area centroid extracted from geostationary satellite H-8 in southern Western Australia was presented. Additionally, the estimated FSR from the CGFSM was used to verify the performance of the presented methodology.

2. MATERIALS AND METHODS

2.1. Study area and data

Esperance(121°E~122°E, 33°S~34°S) is one of the harbor cities near the South Indian Ocean Coast, Western Australia (Figure. 1). It has a typical Mediterranean climate with a high temperature from October to March of the next year, the average precipitation of the month between 18.9~97.0 mm, the average afternoon relative humidity is around 58%. Esperance has an average elevation of 10.8 m, so the terrain is very flat. In November 2015, three catastrophic bushfires (Cascades, Merivale, the Cape Arid) broke out in the shire of Esperance. It caused the death of four people, and many residents and facilities have been damaged. Also, more than 310,000 hectares crops, shrubs and grasslands were burned. The Cascades and Cape Le Grand fire (the section of blue rectangle in Figure 1) are the main research region in this time with a burned area over 128,000 hectares. The burned plants are crops and grasslands.

Himawari-8 Remote Sensing Data: Himawari-8 Meteorological satellite is one of the Himawari series satellites designed and manufactured by Japan Aerospace Exploration Agency. It is a next generation of geostationary satellite launched on October 7th, 2014 and commenced operations on July 7th, 2015. The H-8 is also the world's first still-weather satellite with the capable of capturing color images[16]. It has 16 observation bands distributed in the range of visible, near infrared and thermal infrared. The Advanced Himawari Imager(AHI) carried by H-8 scans five areas: Full Disk, the Japan Area, the Target Area and two Landmark Areas. More importantly, the observation frequency of H-8 increases to every 10 minutes and the spatial resolution increases to 2 km. Hence, it can obtain 142 images one day, which enhance the ability of continued observation to ground. Data can download from the website of Japan Aerospace Exploration Agency.

Grassland Curing Data (GCD): Grassland curing is the dead fraction of grassland expressed as a percentage, strictly by dried weight[17]. Curing has a great influence on the rate of fire propagation in the grassland and is also an important

input of the fire spread model. There are two types of grassland curing data products covered Australia. One is based on Bushfire CRC Project A1.4, and the other is based on the Victorian Country Fire Authority[17] (MapVictoria). In two projects, the Moderate Resolution Imaging Spectroradiometer(MODIS) is used to derive the curing data, with the time and spatial resolution are 8-days and 500-m grid, respectively. The difference between two products is the number of sites which are used to train the algorithms. The MapVictoria has more adequate training samples, reaches to 200, while the Bushfire CRC algorithm only has 25 training samples. The band information of H-8 is similar to that of Modis which is used to obtain Curing data. Therefore, MapVictoria's algorithm is selected to retrieve the Curing data based on H-8 data in this paper.

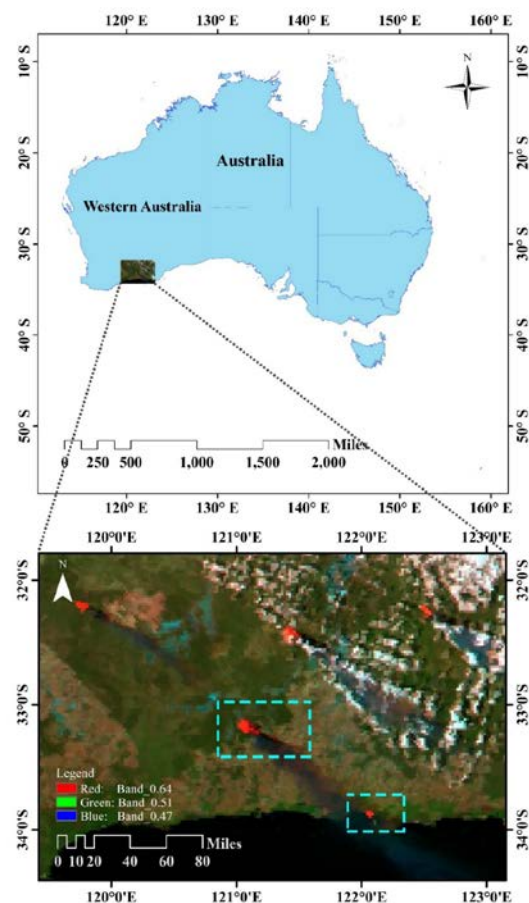


Figure 1. Location of the study area

Meteorological Observation Data: Meteorological data are important factors for both empirical and physical models. In this study, the instantaneous hourly Land-Based Station weather observation data (Wind direction& speed, Temperature, Relative humidity) downloaded from National Climatic Data Center (NCDC) (<https://www.ncdc.noaa.gov/>) were used as the input parameters of CGFSM. The data of nearest four stations were adopted in this research. The stations are as follows: ESPERANCE (No.946380),

ESPERANCE AERO (No.956380), SALMON GUMS RES. STN (No.956390), MUNGLINUP WEST (No.956440). They provided the weather observation data at the time 3:00, 4:00, 6:00, 7:00, 9:00 and 10:00 UTC every day.

2.2. Hotspots detection

In this study, the hotspots detection algorithm which developed by Guang et al. [14] was used. It contains three parts: Detecting Potential Hotspot, Water Masking and Cloud Masking. The criterions are shown in equation (1) - (3). A time series hotspots data was achieved using this algorithm. Meantime, time series burned area were also got. Then, those data were used for fire spread rate extraction after processed.

$$(Z_{T_{3.9}} > 0.8) \text{ and } (Z_{T_{3.9}} - Z_{T_{11.2}} > 1.5) \quad (1)$$

$$(A_{2.3} > 0.05) \quad (2)$$

$$(A_{0.64} + A_{0.86} < 1.2) \text{ and } (T_{12.4} < 265K) \text{ and} \quad (3)$$

$$((A_{0.64} + A_{0.86} < 0.7) \text{ or } (T_{12.4} > 265K))$$

Where $A(\cdot)$ denote the albedo value, $Z(\cdot) = \frac{(\cdot) - \text{mean}(\cdot)}{\text{std}(\cdot)}$,

$\text{mean}(\cdot)$ and $\text{std}(\cdot)$ denote the average and standard deviation of (\cdot) within our study area where $T_{3.9} < 360K$ in daytime.

2.3. Fire Spread Rate estimation from CGFSM

To evaluate the proposed method performance, the CSIRO Grassland Fire Spread Model [18] was also used to estimate FSR. It is an empirical model for estimating the grassland fire spread rate in undisturbed and cut/grazed pastures. The inputs of the model include 10-m open wind speed (km/h) (U_{10}), the dead fuel moisture content (% oven-dry weight basis) (MC) and the degree of grass curing (%) (C). The value of MC can be computed from the temperature ($^{\circ}C$) (T) and the relative humidity (%) (RH). Equations (4) - (7) display the composition of the model.

$$MC = 9.58 - 0.205 * T + 0.138RH \quad (4)$$

$$\phi M = \begin{cases} 0.684 - 0.034 * MC, MC \geq 12\%, U_{10} < 10 \text{ km/h} \\ 0.547 - 0.0228 * MC, MC \geq 12\%, U_{10} \geq 10 \text{ km/h} \end{cases} \quad (5)$$

$$\phi C = \frac{1.036}{1 + 103.99 \exp(-0.0996(C - 20))} \quad (6)$$

$$FSR = \begin{cases} (0.054 + 0.269 U_{10}) \phi M \phi C, U_{10} \leq 5 \text{ km/h} \\ (1.4 + 0.838 (U_{10} - 5)^{0.844}) \phi M \phi C, U_{10} > 5 \text{ km/h} \end{cases} \quad (7)$$

2.4. Fire Spread Rate extraction from Himawari-8

In this paper, a method based on the movement rate of burned area centroid is presented. Fire will spread outwards at normal speed in the form of an ellipse when there is no wind during the firing according to the discipline of fire propagation, which means there is no movement of the centroid of burned area. Therefore, as Figure 2 shows, we can

assume that the fire spread rate can be represented by the rate of burned area centroid movement in the windy situation. The FSR can be calculated by extracting the distance of the centroid movement. As is shown in equation (8).

$$V_{(i,i+1)} = \frac{D_{(i,i+1)}}{T_r} \quad (8)$$

where $D(i, i+1)$ is the distance of the centroid move from time i to time $i+1$, T_r is the time resolution of H-8, and V is the FSR.

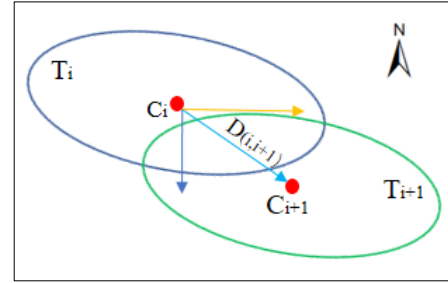


Figure 2. A simple map for centroid movement

3. RESULTS

In this paper, a total of eighteen Himawari-8 images were downloaded to extract fire spread rate in Esperance at the time of 3:00, 4:00, 6:00, 7:00, 9:00 and 10:00 UTC, on November 17th, 2015. The time series hotspots were firstly extract from the H-8 data using the Guang's algorithm. The burned area data were got from the hotspots. Then, by extracting the centroid geographical coordinates of each burned area, the FSR were calculated. The FSR estimated from the CGFSM model were set as the benchmark to validate the FSR estimated from H-8 data. Figure 3 shows the relationship between FSR_H-8 and FSR_CGFSM. It indicated that FSR_H-8 extracted from Himawari-8 have a good association with FSR_CGFSM. The R^2 is 0.76 and RMSE is $0.5 \text{ m} \cdot \text{s}^{-1}$.

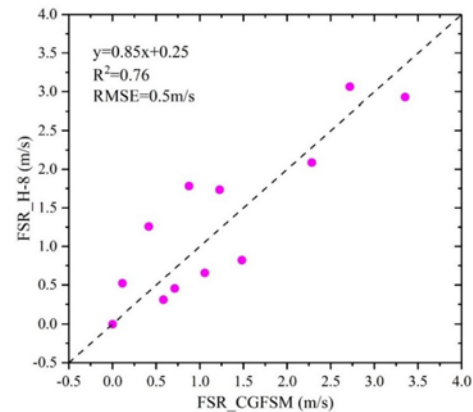


Figure 3. The results of FSR between H-8 vs. CGFSM

4. CONCLUSIONS

Extracting real-time FSR from remote sensing data is paramount to fire rescue and prevention. The launch of the

geostationary H-8 provided the potential application for this end. In this study, the real-time FSR were extracted based on the centroid movement of the H-8 time-series burned area data. The case study of FSR extraction was carried on the two Esperance fires. The result has a $R^2 = 0.76$ and a $RMSE = 0.50 \text{ m} \cdot \text{s}^{-1}$ compared to the benchmark FSR from the CGFSM model. This study also demonstrated the good performance of using geostationary satellite data in real-time wildfire detection.

5. ACKNOWLEDGMENTS

This work was supported by the National Natural Science Foundation of China (Contract No. 41471293 & 41671361), the Fundamental Research Fund for the Central Universities (Contract No. ZYGX2017KYQD195), the Fund Project of Sichuan Provincial Academician (Expert) Workstation (Contract No. 2016YSGZZ01) and the Science and Technology Plan Projects of Sichuan Province (Contract No. 2017GZ0303).

6. REFERENCES

- [1] D. X. Viegas, L. M. Ribeiro, M. T. Viegas, L. P. Pita, and C. Rossa, *Impacts of Fire on Society: Extreme Fire Propagation Issues*. Springer Berlin Heidelberg, 2009, pp. 97-109.
- [2] X. Quan, B. He, M. Yebra, C. Yin, Z. Liao, and X. Li, "Retrieval of forest fuel moisture content using a coupled radiative transfer model," *Environmental Modelling & Software*, vol. 95, pp. 290-302, 2017.
- [3] T. V. Loboda and I. A. Csizsar, "Reconstruction of fire spread within wildland fire events in Northern Eurasia from the MODIS active fire product," *Global and Planetary Change*, vol. 56, no. 3-4, pp. 258-273, 2007.
- [4] M. P. Plucinski, A. L. Sullivan, C. J. Rucinski, and M. Prakash, "Improving the reliability and utility of operational bushfire behaviour predictions in Australian vegetation," *Environmental Modelling & Software*, vol. 91, pp. 1-12, 2017.
- [5] X. Quan *et al.*, "A radiative transfer model-based method for the estimation of grassland aboveground biomass," *International Journal of Applied Earth Observation and Geoinformation*, vol. 54, pp. 159-168, 2017.
- [6] M. G. Cruz *et al.*, "Evaluation of the predictive capacity of dead fuel moisture models for Eastern Australia grasslands," *International Journal of Wildland Fire*, vol. 25, no. 9, p. 995, 2016.
- [7] M. G. Cruz and M. E. Alexander, "Uncertainty associated with model predictions of surface and crown fire rates of spread," *Environmental Modelling & Software*, vol. 47, pp. 16-28, 2013.
- [8] X. Quan, B. He, and X. Li, "A Bayesian Network-Based Method to Alleviate the Ill-Posed Inverse Problem: A Case Study on Leaf Area Index and Canopy Water Content Retrieval," *IEEE Transactions on Geoscience and Remote Sensing*, vol. 53, no. 12, pp. 6507-6517, 2015.
- [9] D. A. Stow, P. J. Riggan, E. J. Storey, and L. L. Coulter, "Measuring fire spread rates from repeat pass airborne thermal infrared imagery," *Remote Sensing Letters*, vol. 5, no. 9, pp. 803-812, 2014.
- [10] E. Pastor, A. Àgueda, J. Andrade-Cetto, M. Muñoz, Y. Pérez, and E. Planas, "Computing the rate of spread of linear flame fronts by thermal image processing," *Fire Safety Journal*, vol. 41, no. 8, pp. 569-579, 2006.
- [11] Fatkhuroyan, T. Wati, and A. Panjaitan, "Forest fires detection in Indonesia using satellite Himawari-8 (case study: Sumatera and Kalimantan on august-october 2015)," *IOP Conference Series: Earth and Environmental Science*, vol. 54, p. 012053, 2017.
- [12] W. Xu, M. J. Wooster, T. Kaneko, J. He, T. Zhang, and D. Fisher, "Major advances in geostationary fire radiative power (FRP) retrieval over Asia and Australia stemming from use of Himawari-8 AHI," *Remote Sensing of Environment*, vol. 193, pp. 138-149, 2017.
- [13] C. Wickramasinghe, S. Jones, K. Reinke, and L. Wallace, "Development of a Multi-Spatial Resolution Approach to the Surveillance of Active Fire Lines Using Himawari-8," *Remote Sensing*, vol. 8, no. 11, p. 932, 2016.
- [14] G. Xu and X. Zhong, "Real-time wildfire detection and tracking in Australia using geostationary satellite: Himawari-8," *Remote Sensing Letters*, vol. 8, no. 11, pp. 1052-1061, 2017.
- [15] W. W. Hou *et al.*, "Near real time SST retrievals from Himawari-8 at NOAA using ACSPO system," vol. 9827, p. 98270L, 2016.
- [16] K. Bessho *et al.*, "An Introduction to Himawari-8/9-Japan's New-Generation Geostationary Meteorological Satellites," (in English), *Journal of the Meteorological Society of Japan*, vol. 94, no. 2, pp. 151-183, 2016.
- [17] D. Martin, T. Chen, D. Nichols, R. Bessell, S. Kidnie, and J. Alexander, "Integrating ground and satellite-based observations to determine the degree of grassland curing," *International Journal of Wildland Fire*, vol. 24, no. 3, p. 329, 2015.
- [18] Cheney N P, Gould J S, and C. W. R., "Prediction of Fire Spread in Grasslands," *International Journal of Wildland Fire*, vol. 8, no. 1, pp. 1-13, 1998.